ORIGINAL ARTICLE

WILEY

Physico-chemical and biological characterization of a new bovine bone mineral matrix available for human usage

Pablo Galindo-Moreno DDS, PhD [1,2] | Natividad Martín-Morales BS [1,2,3,4] |
Allinson Olaechea DDS, MS [1,2,5] | Pedro Hernández-Cortes MD, PhD [2,6] |
Cristobal Verdugo-Escamilla BDC, MSc, PhD [7] | Francisca Martinez-Ruiz BS, PhD [7] |
Ana Belen Carrillo-Galvez PhD [1,2] | Francisco O'Valle MD, PhD [2,3,8] |
Miguel Padial-Molina DDS, PhD [1,2]

[1]Department of Oral Surgery and Implant Dentistry, School of Dentistry, University of Granada, Granada, Spain

[2]Instituto de Investigación Biosanitaria, ibs. GRANADA, Granada, Spain

[3]Department of Pathology, School of Medicine, University of Granada, Granada, Spain

[4]PhD Program in Biomedicine, University of Granada, Granada, Spain

[5]PhD Program in Clinical Medicine and Public Health, University of Granada, Granada, Spain

[6]Department of Surgery, School of Medicine, University of Granada, Granada, Spain

[7]Instituto Andaluz de Ciencias de la Tierra (CSIC-University of Granada), Granada, Spain

[8]Institute of Biopathology and Regenerative Medicine (IBIMER, CIBM), University of Granada, Granada, Spain

Correspondence
Pablo Galindo-Moreno, DDS, PhD, School of Dentistry, Campus Universitario de Cartuja, s/n 18071, Granada, Spain.
Email: pgalindo@ugr.es

Funding information
Junta de Andalucía

Abstract

Background: Anorganic bovine bone has been deeply studied for bone regeneration in the oral cavity. Different manufacturing processes can modify the final composition of the biomaterial and the responses that induce.

Aim: To evaluate the physico-chemical characteristics of a bovine bone mineral matrix and the clinical, radiographical, histological, and mRNA results after using it for maxillary sinus floor augmentation in humans.

Materials and Methods: First, the physical–chemical characteristics of the biomaterial were evaluated by X-ray powder diffraction, X-ray fluorescence, and electron microscopy. A frequently used biomaterial with the same animal origin was used as comparator. Then, a clinical study was designed for evaluating clinical, radiographical, histological, and mRNA outcomes. Patients in need of two-stage maxillary sinus floor augmentation were included in the study. Six months after the grafting procedure, a bone biopsy was collected for evaluation.

Results: In terms of physico-chemical characteristics, no differences were found between both biomaterials. Clinically, 10 patients were included in the study. After 6 months, clinical and radiographical data showed adequate outcomes for allowing implant placement. Histological, immunohistochemical and mRNA analyses showed that the biomaterial in use provides biological support to induce responses similar to those of other commonly used biomaterials.

Conclusion: Bovine bone mineral matrix (Creos™ Xenogain) used as a single material for maxillary sinus floor augmentation shows adequate biological, clinical, and radiological outcomes. In fact, the results from this study are similar to those reported in the literature for another bovine bone-derived biomaterial with whom it shares composition and micro- and nanoscale characteristics.

Summary Box

What is known
- Anorganic bovine bone has been deeply studied for bone regeneration in the oral cavity.
- Different manufacturing processes can modify the final composition of the biomaterial and the responses that induce.

What this study adds
- Bovine bone mineral matrix (Creos™ Xenogain) used as a single material for maxillary sinus floor augmentation shows adequate biological, clinical, and radiological outcomes.

1 | INTRODUCTION

The research model based on sinus floor augmentation carried out in two surgical phases brings great benefits to the scientific community for evaluating the behavior of bone grafts in humans.[1] This model usually provides dimensional stability to the graft. Thus, the graft will be out of the influence of distorting factors such as oral bacteria or mastication. It will also be surrounded by a fully osteogenic environment where mesenchymal stem cells do not usually find cellular competition from other tissues as occurs in the post-extraction socket model. There is no doubt that the greatest advantages of this clinical research model are (1) the possibility to obtain histologic data from human bone, and (2) the possibility of translational research to any other part of the human bone anatomy, thus, applicable in other disciplines such as Traumatology.

The development of the industry continuously provides us with innovations and new materials that promise improved clinical utility with respect to their competitors. However, in many cases, such innovations reach the clinician with very little scientific validation and knowledge that supports their use. Many times, these products only change names due to company policies, such as acquisition of product lines between companies. Their legal permits for marketing and use in humans are frequently only based on theoretical comparisons with similar products. However, we cannot forget that each product undergoes different manufacturing processes that define its physical–chemical characteristics. Therefore, despite showing similarities with others, its subsequent biological behavior may be different.[2]

In this sense, the anorganic bovine bone, specifically Bio-Oss®, from Geistlich Pharma AG, has turned out to be the most researched biomaterial, and endorsed by the literature. In some way, it has become the standard comparator. Recently, one of the most prestigious multi-national companies in the dental sector, Nobel Biocare, has launched a line of products in regeneration. Among them, a bone graft of bovine origin stands out. However, to our knowledge, there is hardly any independent scientific literature to support its use and report its regenerative outcomes.

It is our objective in the present work to characterize the particles of this bovine bone graft in terms of physical–chemical properties,

and to understand the mechanisms of bone repair and maturation after using this biomaterial in humans, considering clinical, radiological, ultrastructural, histomorphometric, histological, immunohistochemical, and gene expression data. We will use the sinus floor augmentation as research model.

2 | MATERIALS AND METHODS

2.1 | Physico-chemical characterization

First, a sample of the bovine bone mineral matrix (Creos™ Xenogain, small granules 0.2–1.0 mm; reference: N1140-B, lot code: B211251B) was used for evaluating the physico-chemical characteristics. The results were compared to those of a sample of spongious bovine bone substitute (Bio-Oss®, small granules 0.25–1 mm, reference: 30643.3/500610, lot code: 82100866). Physico-chemical characterization was carried out at the Fluorescence and X-ray Diffraction Units of the Instituto Andaluz de Ciencias de la Tierra (IACT, CSIC-UGR), and at the Electron Microscopy Units of the Centre for Scientific Instrumentation (UGR).

2.1.1 | Powder X-ray diffraction analysis

Powder X-ray diffraction (PXRD) patterns were acquired on a Bruker D8 Advance Series II Vario diffractometer (Bruker, AXS, Karlsruhe, Germany) using Cu-K$_{\alpha1}$ radiation ($\lambda = 1.5406$ Å) at 40 kV and 40 mA. Diffraction patterns were collected over 2Θ range of 5–60 and using a continuous step size of 0.02 and a total acquisition time of 1 h. The software used for data analysis was Diffrac.EVA v5.0 and TOPAS v6.0 (Bruker, AXS, Karlsruhe, Germany).

2.1.2 | X-ray fluorescence analysis

Chemical composition was determined by X-ray fluorescence (XRF) in fused beads prepared by weighting representative powder of

each sample (∼1 g) with dilithium tetraborate flux and fusing the mixture at 1000°C for 15 min. The analyses were performed using a BRUKER S4 Pioneer XRF instrument equipped with 4 kW wavelength dispersive X-ray fluorescence spectrometer (WDXRF) and an Rh anode X-ray tube (60 kV, 150 mA). Precision (% relative SD), measured by repeated analyses of international reference materials was better than 3%. The LOI was determined at a temperature of 900°C.

2.1.3 | Electron microscopy analyses

For scanning electron microscopy analysis, samples were coated with carbon and observed using a VPSEM Zeiss SUPRA40VP microscope equipped with an energy dispersive X-ray (EDX) detector system. For transmission electron microscopy analysis, sample powder was deposited on carbon-film-coated copper grids and observed using a FEI TITAN G2 60–300 microscope with a high brightness electron gun (X-FEG) operated at 300 kV and equipped with a Cs image corrector CEOS. For analytical electron microscopy (AEM), a SUPER-X silicon-drift windowless EDX detector was used. EDX maps were also collected for determining major element distribution.

2.2 | Clinical study

To respond to our goal in terms of clinical outcomes, a consecutive case-series study was conducted following the recommendations by the STROBE guidelines. The protocol was reviewed and approved by the Ethics Committee for Human Research of the University of Granada, Spain (823/CEIH/2019). All patients signed an informed consent.

2.2.1 | Settings and locations

Surgical procedures were conducted at the Research Clinics of the School of Dentistry, University of Granada. Laboratory techniques were performed at the Department of Pathology and the Laboratory of Oral Health and Regeneration (University of Granada).

2.2.2 | Participants

Patients who were referred to receive implants in the maxillary posterior area were screened for inclusion in the study. Patients were included if they were in need of maxillary sinus floor augmentation with less than 5 mm of residual bone height. Exclusion criteria were prior medical condition affecting bone metabolism (such as bisphosphonate or osteoporosis), smokers of more than 10 cigarettes per day and any other condition that could affect the surgical procedure. None of the patients who met the initial requirements presented any of the criteria to be excluded.

2.2.3 | Interventions

Maxillary sinus augmentation was performed following a surgical lateral window approach. The mesio-distal dimension of the window was conditioned by the number of implants to be placed but considering two principles: (1) influence of the window size on the maturation of the graft[3] and (2) Schneiderian membrane deformation properties.[4] Then, bovine bone mineral matrix (Creos™ Xenogain [Nobel Biocare Services AG, Switzerland], 250–1000 μm particle size) was used as graft biomaterial, hydrated in saline solution. Immediately after placing the graft, a resorbable porcine-derived membrane (Creos™ Xenoprotect; Nobel Biocare Services AG, Switzerland) was used to cover the sinus window. Finally, 3/0 surgical silk (Laboratorio Aragó, Barcelona, Spain) was used to suture and reposition of the soft tissues. Antibiotics (amoxicillin 1 g every 8 h for the period of 7 days) and pain killers (ibuprofen 600 mg every 8 h during 4 days and metamizole 575 mg every 8 h on demand) were prescribed for each patient. Sutures were removed after 1 week.

After 6 months of graft healing, dental implants were placed in the area. To perform the implant bed, 3.5 × 22 mm trephines (Salvin Dental Specialties, Inc, Charlotte, NC, USA) were used to collect bone biopsies. The biopsies were immediately immersed in a 10% formalin solution for histologic, histomorphometric, and immunohistochemical evaluations. An additional biopsy per patient was immersed in Trizol™ for messenger RNA (mRNA) analyses. When possible, a third biopsy was obtained and preserved in 2.5% glutaraldehyde solution for transmission electron microscopy (TEM). After using the trephine, the final drills of the implant system (AstraTech Implant System EV, Dentsply Sirona Implants) were used, and the corresponding implants were placed in site.

All maxillary sinus floor augmentation surgeries and implant placements were conducted by the same surgeon (P.G.-M.).

2.2.4 | Outcomes measures

The primary outcome measure of the current study was radiographic bone height gained 6 months after the maxillary sinus floor augmentation procedure, given that this parameter is critical for the posterior implant placement. Thus, CBCTs from the area before, immediately after and 6 months after the maxillary sinus floor augmentation were obtained. The secondary outcomes were to determine histomorphometric components and the histological properties of the resultant bone. These parameters can explain the biological behavior of the biomaterial. To reach these goals, several histopathological techniques were conducted on the biopsies.

Clinical variables

Age, gender, medications, systemic diseases, tobacco consumption, and alcohol intake were registered from each patient's medical records. Additionally, a full dental exam was conducted to evaluate periodontal status and type of edentulism (total or partial). During the sinus floor augmentation surgery, the mesio-distal width and three measurements of the height of each surgical bony window were recorded, as well as the total volume of biomaterial used.

Radiographic analysis

All radiographic data relevant for the study were evaluated using Horos v4.0.0 RC5 for MacOS Big Sur. First, the height of the residual alveolar crest (RAC), the initial post-op height of the graft (IHG), and the final height of the alveolar crest 6 months after grafting (FH) were analyzed in three positions along the mesio-distal extension of the graft. From those measures, the initial total height (ITH = RAC + IHG), final height gain (FHG = RAC + FH), and vertical change from post-op to 6 months (VC = ITH − FHG) were calculated. Then, the volume of the grafted bone was also analyzed as described previously[5,6] in order to measure initial and final volume and calculate both absolute and relative graft volume resorption.

Finally, the width of the sinus in the bucco-lingual aspect at 5, 10, and 15 mm from the floor of the sinus was also recorded.

All CBCTs were evaluated by an experienced surgeon (M.P.-M.) assisted by a collaborator.

Histopathological analysis

Similar methods to others previously published by our group[6] were followed for conventional morphology. Briefly, biopsies were fixed in 10% formalin buffered solution for 48 h, and then transferred to 70% ethanol. Samples were decalcified during 24 h at 37°C in Decalcifier I (Surgipath Europe Ltd., Peterborough, UK). Hematoxylin–eosin and Masson's trichrome stains were performed and observed under a BX42 light microscope (Olympus Optical Company, Ltd., Tokyo, Japan) with a 40× objective for the quantification of relevant cells per mm^2. 10× images were also captured with a CD70 camera (Olympus Optical Company, Ltd., Tokyo, Japan) attached to the microscope for the quantification of percentages of mineralized and non-mineralized tissue, and remnant biomaterial using ImageJ software (http://imagej.nih.gov/ij/). An experienced researcher performed these evaluations (N.M.-M.).

Immunohistochemical analysis

Immunohistochemical techniques were conducted to visualize the expression, location, and number of positive cells per mm^2 for osteocytes (CD44), osteoblasts (CD56), osteoclasts (TRAP), mesenchymal stromal cells (MSI1), leukocytes (CD45), and monocytes (CD68). Number of vessels (CD34), osteoid lines, and expression of osteopontin in a 0–3 scale were also quantified. For that, after deparaffinizing and rehydrating slides, they were treated in a pretreatment thermal PT module (Thermo Fisher Scientific Inc., Waltham, MA, USA) with 1 mM EDTA buffer (pH 8) for 20 min at 95°C. Then, a predetermined concentration of each primary antibody was applied for 1 h at room temperature. Staining was visualized using a micropolymer conjugated with peroxidase and diaminobenzidine in an automated immunostainer (Autostainer 480S, Thermo Fisher Scientific Inc.). All antibodies were purchased from the same company (Vitro-Master Diagnóstica, Granada, Spain).

Transmission electron microscopy

Graft biopsies fixed in 2.5% glutaraldehyde solution were decalcified as described above. Then, they were post-fixed in 1% OsO$_4$ at 4°C for 2 h, washed and dehydrated in acetone. Semi-thin sections (∼70 nm thick) were obtained by embedding the samples in Epon and using a Reichert Jung Ultracut ultramicrotome (Leica, Wetzlar, Germany). Ultrathin sections were then re-stained with lead citrate and uranyl acetate and analyzed on a Zeiss Libra 120 TEM (Carl Zeiss AG, Oberkochen, Germany).

mRNA analysis

Biopsies were kept in Trizol™ reagent at −80°C until processing them, starting with homogenization in a tissue blender. Trizol™ Plus RNA Purification kit (Invitrogen, Grand Island, NY, USA) was used for isolating the total RNA. Then, 30 μL of cDNA with 1 μg of RNA were generated with PrimeScript RT Master Mix (Takara Bio Europe, Saint-Germain-en-Laye, France). Then, 2 μL of each sample per replicate (a total of two replicates per sample) were used for quantitative real-time PCR using SYBR Premix Ex Taq II (Takara Bio Europe, Saint-Germain-en-Laye, France) using the rt-PCR primers previously published.[6] The 2^{-ddCt} method was used to calculate gene expression levels in relation to glyceraldehyde-3-phosphate dehydrogenase (GAPDH). As no control is present in this study design, individual expression in each gene was calculated relative to the overall expression.

2.2.5 | Statistical analysis

Analyses and graphical representations were made on GraphPad Prism 7.0a, Microsoft Excel 16.59, and IBM® SPSS® Statistics 28.0.1.0 for Mac OS X. Data are presented as percentages and means (standard deviation) if they are categorical or continuous variables, respectively. Differences between areas of native and grafted bone and between radiographic before and after measures were evaluated by non-parametric Wilcoxon matched-pairs signed-rank tests. Pearson correlation coefficient was used to evaluate the association between clinical and histological variables. p values of 0.05 were considered the limit for statistical significance.

3 | RESULTS

3.1 | Biomaterials characterization

3.1.1 | Powder X-ray diffraction analysis

The PXRD data analysis of Bio-Oss® and Creos biomaterials reveals they are equivalent materials from the structural and microstructural points of view. As can be seen in Figure 1, the PXRD patterns are equivalent, and no difference can be observed between both biomaterials. In addition, these patterns are completely overlapped with those of a hydroxyapatite structure (COD 9010051).

3.1.2 | XRF analysis

XRF analyses have been used to compare the composition of major elements in the studied samples with the aim of identifying potential differences between them. Major components are calcium and
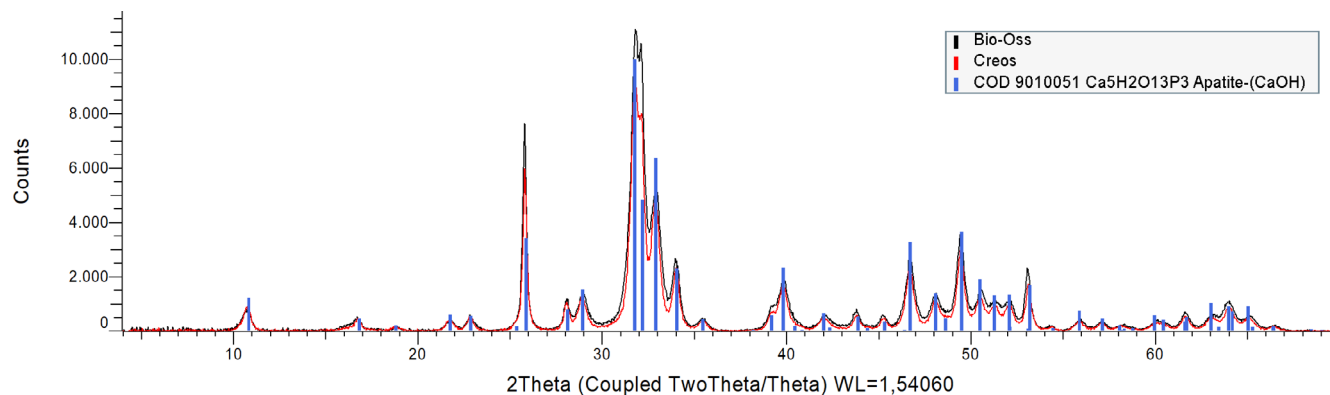
FIGURE 1 Powder X-ray diffraction (PXRD) analysis showing that both biomaterials are equivalent and their PXRD patterns are no different. In addition, these patterns are also overlapped with that of hydroxyapatite.

TABLE 1 Major element chemical composition obtained by X-ray fluorescence (in wt%).

	Na_2O	MgO	Al_2O_3	SiO_2	P_2O_5	K_2O	CaO	TiO_2	MnO	Fe_2O_3	LOI
Bio-Oss	0.42	1.05	0.00	0.76	37.55	0.00	51.91	0.01	0.00	0.00	5.95
Creos	0.24	1.08	0.01	0.78	38.45	0.00	52.54	0.01	0.00	0.00	3.99

phosphorous as expected from a hydroxyapatite. Major elements contents are presented in Table 1. No significant differences have been identified in terms of composition.

3.1.3 | Scanning microscopy analysis

Electron microscopy observations demonstrate that morphology and composition of the studied samples are also similar. Figure 2 (SEM + TEM) shows the morphologies identified in both samples at different observation scales. At the microscale, sample particles have been measured under the SEM and particle size is similar in both materials. SEM–EDX analyses have also reported the same composition corresponding to hydroxyapatite. At the nanoscale (Figure 2C,F) also similar structures and nanocrystals are observed.

3.1.4 | High-resolution electron microscopy analysis

High-resolution electron microscopy observations further demonstrate that morphology and composition of the studied samples are also similar (Figure 2G–J). A detailed TEM-AEM study of hydroxyapatite crystals has also shown similar EDX spectra and maps in all cases, supporting similarity at the nanoscale.

3.2 | Clinical study

3.2.1 | Clinical variables

The current study spanned from June 2019 (first patient included) until July 2021 (last biopsy collected). A total of 10 patients were included in the study, although only 9 were evaluated because one of them was diagnosed with spleen lymphoma soon after the sinus floor augmentation surgery. Thus, he was excluded from all analyses. Out of the remaining nine patients, four were females (44.44%). Their average age was 53 years (40–64, minimum and maximum, respectively). None of them was smoker nor consumed alcohol regularly. Four patients had history of severe periodontal disease, three had moderate periodontal disease, and two were periodontally healthy. Five of the sinuses subjected to the floor augmentation were the right ones. Only two patients were completely edentulous. Healing was uneventful in all cases with no adverse events.

3.2.2 | Radiological results

Neither graft height at the mesial, central, and distal sites nor total volume of the grafted area changed significantly from the post-operative evaluation until 6 months later ($p = 0.652$, $p = 0.461$, $p = 0.410$, and $p = 0.219$, respectively). In fact, vertical graft change was less than 1 mm in all three sites, while volume loss was quite small, on average, 5.49%.

All radiographic measurements are summarized in Figure 3 and Table S1.

3.2.3 | Histopathological results

Table 2 shows the percentual area of the different tissue compartments, expressed as mean % (SD). Figure 4A shows a representative image of the areas indicated. As shown, the comparison between pristine and grafted bone demonstrates differences in terms of mineralized and non-mineralized areas, being significantly
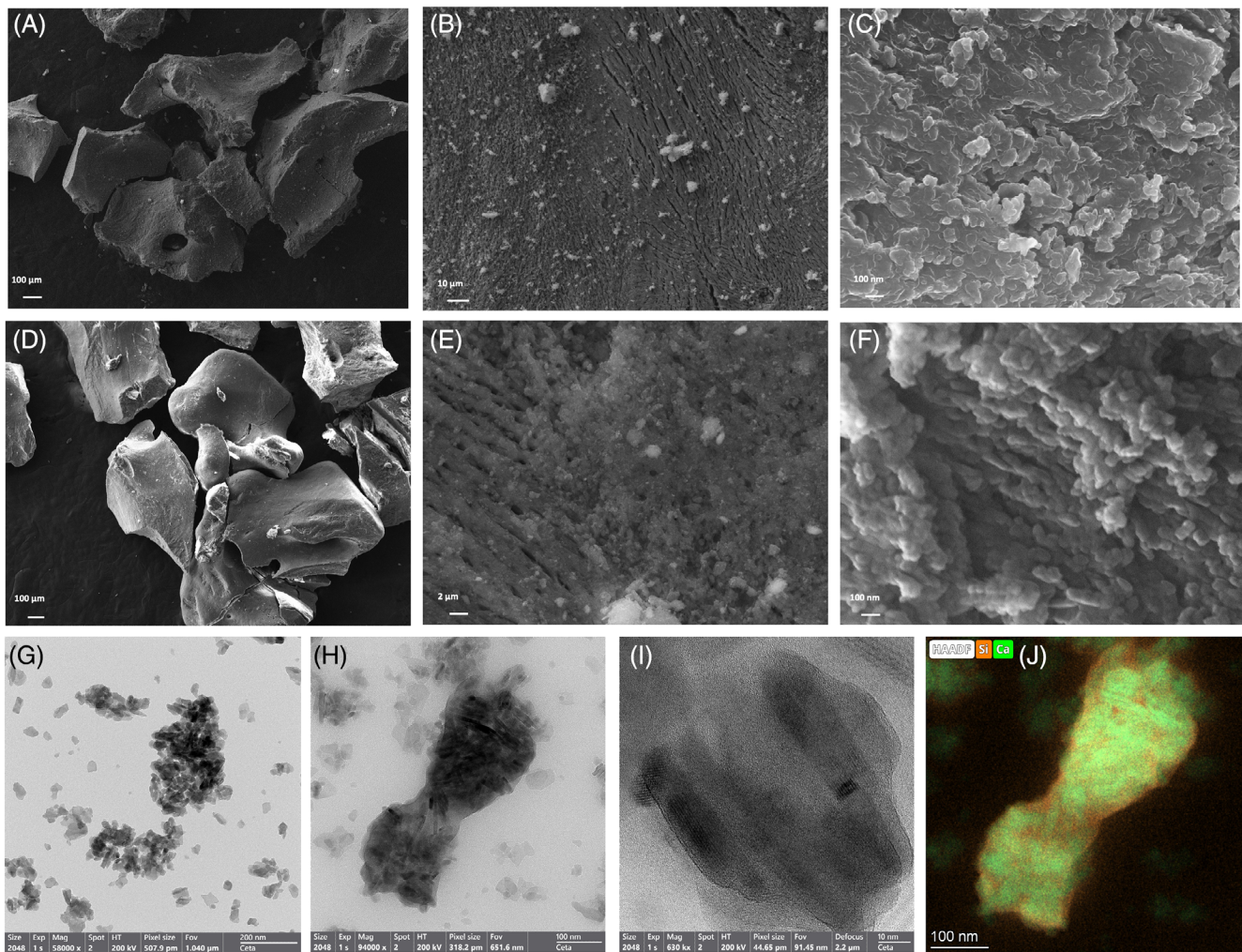
FIGURE 2 Different scale observations of Bio-Oss (A–C) and Creos (D–F) particles are presented, showing similar characteristics at the micro and nanoscale. High-angle annular dark field (HAADF) STEM images from Creos (G) and Bio-Oss (H–I) further indicate similar morphology and nature of the hydroxyapatite particles, as also shown in EDX maps. A representative example (Bio-Oss) has been selected showing the distribution of Si and Ca (J).

lower in both cases in the grafted area ($p = 0.016$ and $p = 0.047$, mineralized and non-mineralized tissue, pristine bone versus grafted area, respectively; Wilcoxon matched-pairs signed rank test). If the total bone core is considered as a representation of the area interacting with the future implant, the percentage of non-mineralized tissue is 25.46 (6.75), compared to a total mineralized tissue compartment of 39.13 (10.71)% and 39.84 (9.79)% of remaining biomaterial.

As expected, although not statistically significant, the number of osteoid lines in pristine bone was lower than in the grafted area: 3.38 (2.20) versus 5.25 (2.25) ($p = 0.094$; Wilcoxon matched-pairs signed rank test) (Table 3).

No significant correlation was found between histomorphometric data and clinical and radiographic variables, including gender, history of periodontal disease, window dimensions (in mm^2), and sinus width at 10-mm height.

3.2.4 | Immunohistochemical results

Table 3 shows the comparison of number of positively stain cells and vessels per mm^2, as well as the number of osteoid line and the average expression of osteopontin, within pristine, and grafted areas expressed as mean (SD). Figure 4B–E shows representative images of each marker. Overall, the number of cells in the osseous lineage as well as leukocytes, monocytes, and vessels is significantly higher in the grafted area than in pristine bone. Of all the evaluated markers, only MSI1, representative of mesenchymal stromal cells did not show statistically significant differences in expression in pristine versus grafted area ($p = 0.063$; Wilcoxon matched-pairs signed rank test).

No significant correlation was found between immunohistochemical data and clinical and radiographic variables, including gender, history of periodontal disease, window dimensions (in mm^2), and sinus width at 10-mm height.
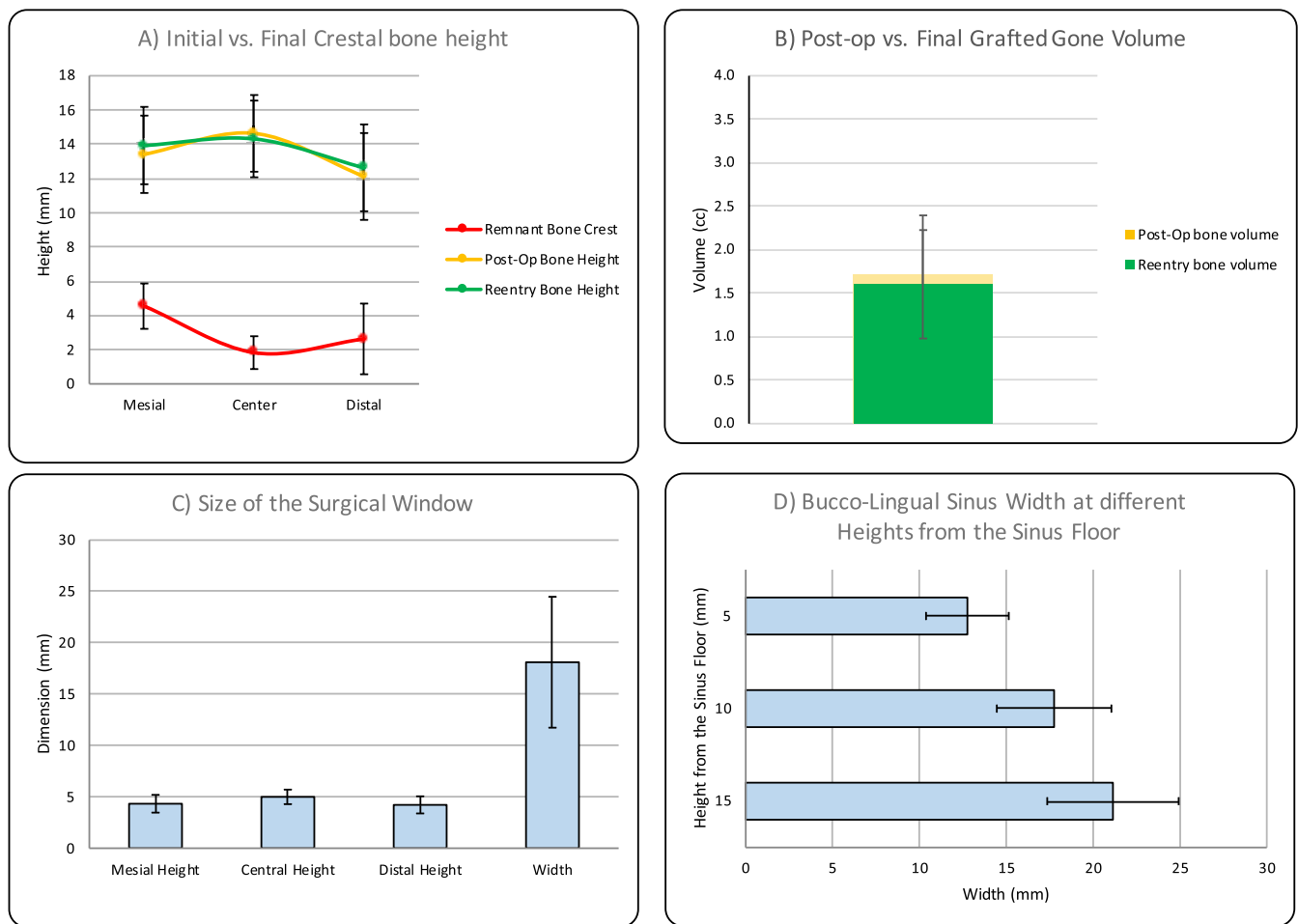
FIGURE 3 (A) Initial (red line), post-operative (yellow line), and final (green line) heights of the alveolar crest at the mesial, central, and distal sites of the grafted area. (B) Post-operative (yellow column) and final (green column) volume of the grafted bone. (C) Height and width of the surgical window. (D) Bucco-lingual width of the sinus cavity at 5, 10, and 15 mm from the floor of the sinus.

TABLE 2 Percentual area of the different tissue compartments.

Tissue compartment	Pristine bone	Grafted area	p-value[a]	Total bone core
Mineralized tissue	62.82 (12.15)	27.46 (6.14)	*0.016*	39.13 (10.71)
Non-mineralized tissue	37.18 (12.15)	19.98 (3.76)	*0.047*	25.46 (6.75)
Remnant biomaterial	NA	52.56 (4.94)	NA	39.84 (9.79)

Note: Data expressed as mean % (SD). Italics indicate statistically significant differences.
[a]Wilcoxon matched-pairs signed rank test comparing pristine versus grafted areas.

3.2.5 | TEM results

Numerous fibroblastic-like cells could be observed near to the new mineralized tissue and osteocytes. In addition, the union between remnant particles of Creos and newly formed mineralized tissue was evident (Figure 5A,B).

3.2.6 | mRNA results

Individual expression of each gene is shown in Table S2. As shown, variability in gene expression is mainly associated to a particular subject, in which the expression of several genes is much higher than that of the other subjects.

4 | DISCUSSION

This study proposed several types of analyses about a recent anorganic bovine bone available in the market, supported and distributed by one of the biggest companies in the dental market. To our knowledge, there are few manuscripts describing this biomaterial from the physical–chemical point of view as well from the biological one. In fact, only one clinical and histological study about lateral ridge

FIGURE 4 (A) Representative image of a trephine biopsy showing the area of pristine and grafted bone. As shown, the remaining biomaterial particles are evenly distributed (*) along the whole vertical dimension. Thus, an also even distribution of new mineralized tissue (+) and non-mineralized areas (#) can be observed. Immunohistochemical detection of (B) osteopontin, (C) leukocytes (CD45), (D) monocytes/macrophages (CD68), and (E) osteoclasts cells (TRAP1) around the remaining Creos particles. White arrows in (B)–(E) point to positivity. (Micropolymer peroxidase conjugated, original magnification 20×; bar scale: 50 μm).
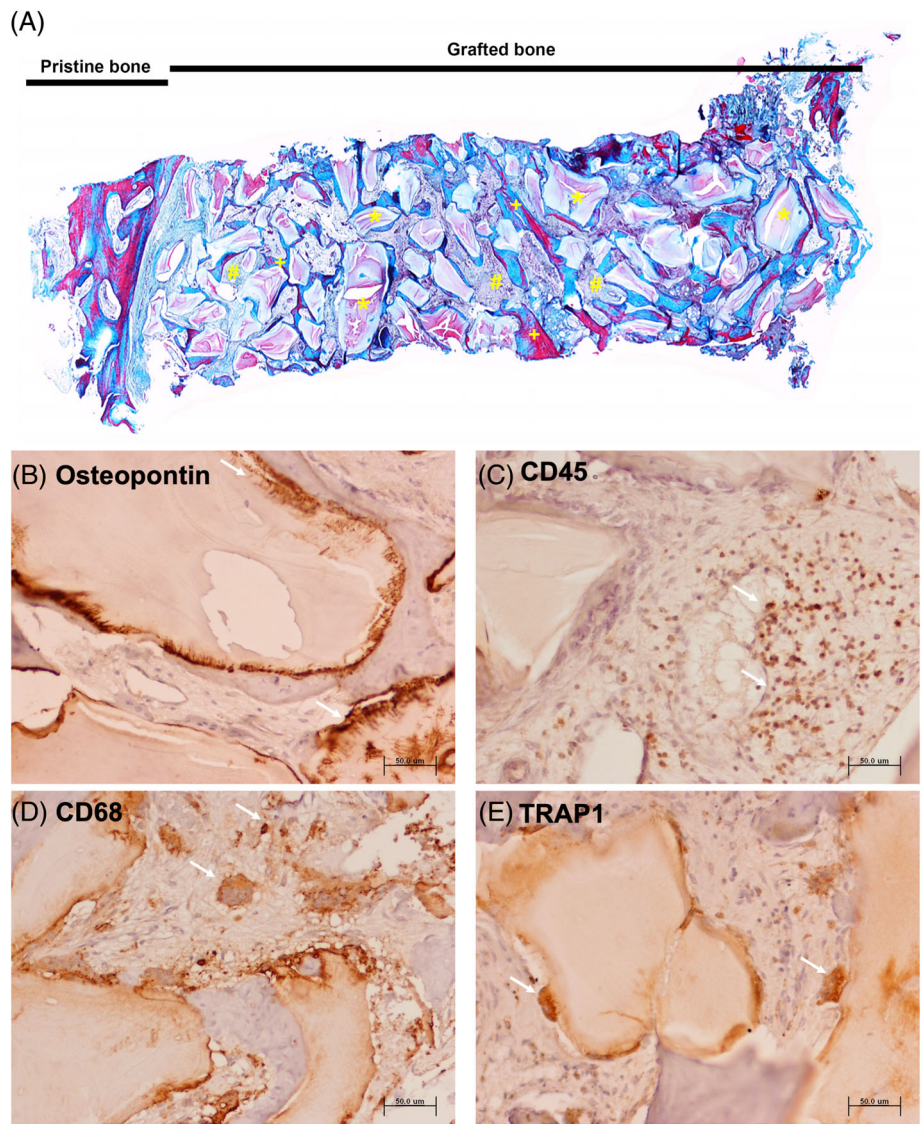
TABLE 3 Comparison of number of positively stain cells, vessels, and osteoid lines per mm² within pristine and grafted areas (expressed as mean [SD]).

|	Pristine bone	Grafted area	*p*-value[a]
CD44 (osteocytes)	108.87 (65.52)	182.80 (92.65)	*0.008*
CD56 (osteoblasts)	0.00 (0.00)	60.93 (34.95)	*0.016*
TRAP (osteoclasts)	0.00 (0.00)	53.76 (50.36)	*0.031*
MSI1 (mesenchymal stromal cells)	84.68 (88.66)	267.03 (213.08)	0.063
CD45 (all leukocytes)	0.00 (0.00)	130.82 (136.49)	*0.031*
CD68 (monocytes)	0.00 (0.00)	107.53 (78.19)	*0.008*
CD34 (endothelial cells, vessels)	26.21 (22.71)	90.50 (40.68)	*0.008*
Osteoid lines	3.38 (2.20)	5.25 (2.25)	0.094
Osteopontin	0.13 (0.35)	1.89 (1.05)	*0.016*

Note: Osteopontin is expressed in average of a 0–3 scale. Italics indicate statistically significant differences.
[a]Wilcoxon matched-pairs signed rank test.

augmentation can be found in the literature, using this biomaterial in humans. Therefore, our first step was to analyze the structural properties of this biomaterial and compare them with the most studied, known, and used bovine bone biomaterial available in the market. For that purpose, a multi-technique approach that includes X-ray diffraction and X-ray fluorescence analyses, as well as TEM and SEM
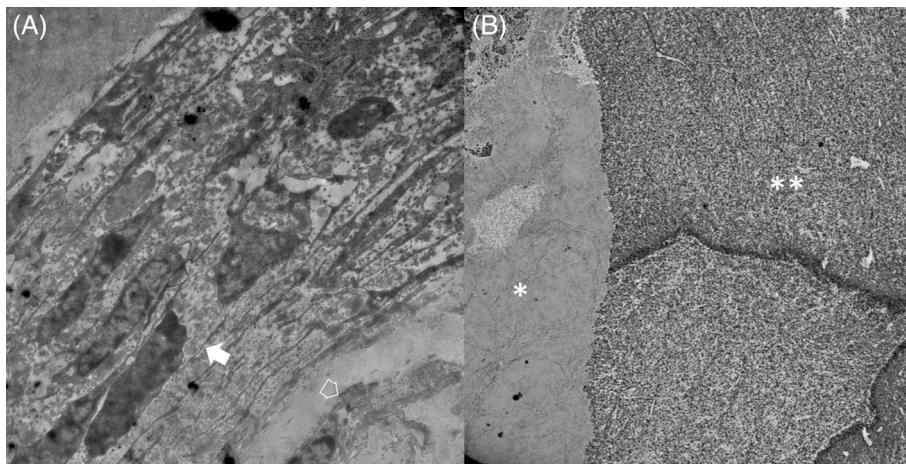
FIGURE 5 (A) Transmission electron microscopy images of clinical samples showing non-mineralized tissue with numerous fibroblastic-like cells (white narrow) near to the new mineralized tissue and osteocyte (empty narrow). Additionally, (B) a close union between remnant particles of newly formed bone (*) and Creos (**) can be observed.

techniques has been used in both biomaterials (Creos™ and Bio-Oss®) in order to analyze similarities or differences between both bovine bone biomaterials. Not surprisingly, both biomaterials exhibited the same structure and characteristics at different observation scales, from micro to nanometer scale (Figures 1 and 2), and also similar chemical composition (Table 1). However, because of the different manufacturing processes, it can be suggested that the biological behavior might be different, as our group has confirmed with materials of human origin.[2] Creos™ Xenogain is reported to be produced through a process in which after the removal of blood, proteins are eliminated by using sodium hypochlorite, instead of the commonly used amine products. After that, the product is irrigated and sintered at over 400°C for 3 h.[7] According to different studies, the use of low temperature for biomaterial sintering positively influences the osteoconductivity of the final product.[8]

Our primary outcome was to analyze radiographic bone height gained 6 months after the maxillary sinus floor augmentation procedure, because this parameter is fundamental for the posterior implant placement. On contrary to recent studies where all used biomaterials showed a relative radiographic graft resorption, a very interesting finding of this study was the absence of Creos™ Xenogain biomaterial resorption in the radiographic evaluation. In fact, after 6 months, a huge histomorphometric presence of remnant biomaterial was still appreciable in the samples (52.56 [4.94]). This remanent biomaterial component percentage is higher than other reported in the literature, using a similar technique, but with a different bovine bone (Bio-Oss®).[6,9–11] These differences cannot be attributed to the anatomical features of the maxillary sinus cavities,[12,13] the amount of remaining crestal bone[14] or to the surgical approaches[3] because these clinical variables were similar to those reported in other manuscripts, using anorganic bovine bone or other different biomaterials[6,10] (Table S1). Consequently, the histomorphometric data showed an important radiological translation. In contrast with the previously cited studies, neither graft height in any anatomical site nor total volume of the grafted area changed significantly from the post-operative evaluation until 6 months later ($p = 0.652$, $p = 0.461$, $p = 0.410$, and $p = 0.219$, respectively). To our knowledge, we cannot find in the literature any bone biomaterial with such a small dimensional change after 6 months

of graft maturation, because in the present study the vertical graft change was less than 1 mm in all three sites, while volume loss was, on average, 5.49%. We contemplate that the histological persistence of this biomaterial is responsible for the radiological height and volumetric graft maintenance. Although this persistence of the biomaterial can be considered a beneficial outcome as it maintains the volume, the potential negative effect that such amount of remnant biomaterial particles might exert on the process of osseointegration needs to be further evaluated. The capacity of the bone surrounding the implant to adapt to new clinical stimulus in the mid/long term also has to be studied.

As expectable, when we compared patients' pristine bone compartments with new grafted bone areas, there were important statistical differences. Remnant Creos™ Xenogain biomaterial persistence conditioned smaller significant percentage of new mineralized and non-mineralized bone (62.82 [12.15] vs. 27.46 [6.14] and 37.18 [12.15] vs. 19.98 [3.76], respectively in pristine vs. grafted areas). However, biological activity looked quite more intense in the grafted area than in the quiescent pristine bone. Undoubtfully, this should be attributed to the absence of remodeling or healing events in the crestal bone. Therefore, even with a smaller non-mineralized component in the grafted areas in comparison with the same component in native areas, cellular and vascular elements were significantly higher. Protein expressed in the bone and biomaterial surface (osteopontin) was also higher in the grafted areas. This could explain the presence of more osteoblasts, osteoclasts and their precursors (monocytes), and osteoid lines in the grafted areas. However, in spite of the high number of new vessels (90.50 [40.68] per mm^2), in fact, one of the highest published in the literature,[6,9,10,15–18] and the high number of mesenchymal stem cells (expressed as MIS1 positive cells) (267.03 [213.08] per mm^2), the final number of cuboid osteoblasts and osteoid lines were limited in comparison with those previous studies using other bovine bone. Moreover, the new mineralized bone component in the grafted area is also reduced in comparison to other biomaterials. Taking together all these data, we could hypothesize that this biomaterial shows a slower bone formation and biomaterial resorption, what would mean a prolonged action in the time.

To our knowledge, only one previous study has been published and made available using this biomaterial for sinus floor augmentation.[7] In another study reported as a poster presentation, the experimental model (lateral ridge augmentation) was different.[19] However, no histological data are reported in any of those manuscripts. Thus, the current manuscript aimed at reporting clinical, radiographical, and histological data from human samples as well as a complete characterization of the biomaterial. Future studies with higher sample sizes should also allow to better explore potential associations between clinical, radiographical, and histological data.

Another goal of this study was to analyze the expression of some genes involved in the bone formation and homeostasis; particularly those related to the pathway of osteo-differentiation of mesenchymal stromal cells. Few manuscripts have shown these parameters[6,10,20] and results are quite similar in all the studies in spite of using different biomaterials. This is easy to explain, because regeneration is conducted by the patient and not by the biomaterial, so it is dependent of the bone area, genetic, and bone function. All these studies are conducted in the same biological area, the posterior superior maxillary bone. So, in our opinion, all these results might be similar in spite of the biomaterial or technique used. In addition, the techniques used for gene evaluation lack spatial localization; thus, the overall expression would seem similar, while possible differences might be washed away.

This study has a main limitation that is the absence of a comparator group. As explained though, it is still important to report on the outcomes of newly available biomaterials for supporting their clinical use with extensive and different data. Future comparisons are granted to confirm our findings.

5 | CONCLUSIONS

Bovine bone mineral matrix (Creos™ Xenogain) used as a single material for maxillary sinus floor augmentation shows adequate biological, clinical, and radiological outcomes, that are, in fact, similar to those reported in the literature for another bovine bone-derived biomaterial (Bio-Oss) with whom it shares composition and micro- and nanoscale characteristics.

AUTHOR CONTRIBUTIONS

Conceptualization: Pablo Galindo-Moreno, Francisco O'Valle, and Miguel Padial-Molina. *Methodology*: Pablo Galindo-Moreno, Cristobal Verdugo-Escamilla, Francisca Martinez-Ruiz, and Francisco O'Valle. *Validation*: Miguel Padial-Molina. *Formal analysis*: Natividad Martín-Morales, Allinson Olaechea, Pedro Hernández-Cortes, Cristobal Verdugo-Escamilla, Francisca Martinez-Ruiz, and Ana Belen Carrillo-Galvez. *Resources*: Pablo Galindo-Moreno and Miguel Padial-Molina. *Data curation*: Francisco O'Valle. *Writing—original draft*: Pablo Galindo-Moreno and Miguel Padial-Molina. *Visualization*: Natividad Martín-Morales, Cristobal Verdugo-Escamilla, Francisca Martinez-Ruiz, Francisco O'Valle, and Miguel Padial-Molina. *Supervision*: Pablo Galindo-Moreno. *Project administration*: Pablo Galindo-Moreno and Miguel Padial-Molina. *Funding acquisition*: Pablo Galindo-Moreno and Miguel Padial-Molina. All authors are involved in investigation and writing—review and editing.

CONFLICT OF INTEREST STATEMENT

The authors declare no conflict of interest, either directly or indirectly, in any of the products listed in the manuscript.

DATA AVAILABILITY STATEMENT

The data that support the findings of this study are available from the corresponding author upon reasonable request.

ORCID

Pablo Galindo-Moreno https://orcid.org/0000-0002-6614-6470
Natividad Martín-Morales https://orcid.org/0000-0003-3540-1085
Allinson Olaechea https://orcid.org/0000-0002-5907-9660
Pedro Hernández-Cortes https://orcid.org/0000-0003-2057-5285
Cristobal Verdugo-Escamilla https://orcid.org/0000-0003-2345-8359
Francisca Martinez-Ruiz https://orcid.org/0000-0002-8301-4453
Ana Belen Carrillo-Galvez https://orcid.org/0000-0002-8361-1469
Francisco O'Valle https://orcid.org/0000-0001-9207-2287
Miguel Padial-Molina https://orcid.org/0000-0001-6222-1341

REFERENCES

1. Avila-Ortiz G, Galindo-Moreno P. Maxillary sinus floor elevation. In: Giannobile WV, Lang NP, Tonetti MS, eds. *Osteology Guidelines for Oral & Maxillofacial Regeneration: Clinical Research Guidelines*. Quintessenz Verlags GmbH; 2014:247-262.

2. Monje A, O'Valle F, Monje-Gil F, et al. Cellular, vascular, and histomorphometric outcomes of solvent-dehydrated vs freeze-dried allogeneic graft for maxillary sinus augmentation: a randomized case series. *Int J Oral Maxillofac Implants*. 2017;32(1):121-127. doi:10.11607/jomi.4801

3. Avila-Ortiz G, Wang HL, Galindo-Moreno P, Misch CE, Rudek I, Neiva R. Influence of lateral window dimensions on vital bone formation following maxillary sinus augmentation. *Int J Oral Maxillofac Implants*. 2012;27(5):1230-1238.

4. Pommer B, Unger E, Sütö D, Hack N, Watzek G. Mechanical properties of the Schneiderian membrane in vitro. *Clin Oral Implants Res*. 2009;20(6):633-637. doi:10.1111/j.1600-0501.2008.01686.x

5. Saito H, Couso-Queiruga E, Shiau HJ, et al. Evaluation of poly lactic-co-glycolic acid-coated β-tricalcium phosphate for alveolar ridge preservation: a multicenter randomized controlled trial. *J Periodontol*. 2021;92(4):524-535. doi:10.1002/JPER.20-0360

6. Galindo-Moreno P, Abril-García D, Carrillo-Galvez AB, et al. Maxillary sinus floor augmentation comparing bovine versus porcine bone xenografts mixed with autogenous bone graft. A split-mouth

randomized controlled trial. *Clin Oral Implants Res*. 2022;33(5):524-536. doi:10.1111/clr.13912

7. Shin SY, Hwang YJ, Kim JH, Seol YJ. Long-term results of new deproteinized bovine bone material in a maxillary sinus graft procedure. *J Periodontal Implant Sci*. 2014;44(5):259-264. doi:10.5051/jpis.2014.44.5.259

8. Rhee SH, Park HN, Seol YJ, Chung CP, Han SH. Effect of heat-treatment temperature on the osteoconductivity of the apatite derived from bovine bone. *Key Eng Mater*. 2006;309-311:41-44. doi:10.4028/www.scientific.net/KEM.309-311.41

9. Galindo-Moreno P, de Buitrago JG, Padial-Molina M, Fernández-Barbero JE, Ata-Ali J, O'Valle F. Histopathological comparison of healing after maxillary sinus augmentation using xenograft mixed with autogenous bone versus allograft mixed with autogenous bone. *Clin Oral Implants Res*. 2018;29(2):192-201. doi:10.1111/clr.13098

10. Galindo-Moreno P, Padial-Molina M, Lopez-Chaichio L, Gutiérrez-Garrido L, Martín-Morales N, O'Valle F. Algae-derived hydroxyapatite behavior as bone biomaterial in comparison with anorganic bovine bone: a split-mouth clinical, radiological, and histologic randomized study in humans. *Clin Oral Implants Res*. 2020;31(6):536-548. doi:10.1111/clr.13590

11. O'Valle F, de Buitrago JG, Hernández-Cortés P, et al. Increased expression of musashi-1 evidences mesenchymal repair in maxillary sinus floor elevation. *Sci Rep*. 2018;8(1):12243. doi:10.1038/s41598-018-29908-3

12. Avila G, Wang HL, Galindo-Moreno P, et al. The influence of the bucco-palatal distance on sinus augmentation outcomes. *J Periodontol*. 2010;81(7):1041-1050. doi:10.1902/jop.2010.090686

13. Stacchi C, Lombardi T, Ottonelli R, Berton F, Perinetti G, Traini T. New bone formation after transcrestal sinus floor elevation was influenced by sinus cavity dimensions: a prospective histologic and histomorphometric study. *Clin Oral Implants Res*. 2018;29(5):465-479. doi:10.1111/clr.13144

14. Avila-Ortiz G, Neiva R, Galindo-Moreno P, Rudek I, Benavides E, Wang HL. Analysis of the influence of residual alveolar bone height on sinus augmentation outcomes. *Clin Oral Implants Res*. 2012;23(9):1082-1088. doi:10.1111/j.1600-0501.2011.02270.x

15. Boeck-Neto RJ, Artese L, Piattelli A, et al. VEGF and MVD expression in sinus augmentation with autologous bone and several graft materials. *Oral Dis*. 2009;15(2):148-154. doi:10.1111/j.1601-0825.2008.01502.x

16. Galindo-Moreno P, Padial-Molina M, Fernández-Barbero JE, Mesa F, Rodríguez-Martínez D, O'Valle F. Optimal microvessel density from composite graft of autogenous maxillary cortical bone and anorganic bovine bone in sinus augmentation: influence of clinical variables. *Clin Oral Implants Res*. 2010;21(2):221-227. doi:10.1111/j.1600-0501.2009.01827.x

17. Galindo-Moreno P, Moreno-Riestra I, Ávila-Ortiz G, et al. Predictive factors for maxillary sinus augmentation outcomes: a case series analysis. *Implant Dent*. 2012;21(5):433-440. doi:10.1097/ID.0b013e3182691959

18. Khosravi N, Maeda A, DaCosta RS, Davies JE. Nanosurfaces modulate the mechanism of peri-implant endosseous healing by regulating neovascular morphogenesis. *Commun Biol*. 2018;1:72. doi:10.1038/s42003-018-0074-y

19. Aleksic Z, Milinkovic I, Lazic ZR, et al. PR546: a multicenter clinical investigation demonstrates bone regeneration in severe horizontal defects in the posterior mandible using creos xenoprotect: interim results. *J Clin Periodontol*. 2018;45(S19):306. doi:10.1111/jcpe.548_12915

20. Caubet J, Ramis JM, Ramos-Murguialday M, Morey MÁ, Monjo M. Gene expression and morphometric parameters of human bone biopsies after maxillary sinus floor elevation with autologous bone combined with Bio-Oss® or BoneCeramic®. *Clin Oral Implants Res*. 2015;26(6):727-735. doi:10.1111/clr.12380

SUPPORTING INFORMATION

Additional supporting information can be found online in the Supporting Information section at the end of this article.

How to cite this article: Galindo-Moreno P, Martín-Morales N, Olaechea A, et al. Physico-chemical and biological characterization of a new bovine bone mineral matrix available for human usage. *Clin Implant Dent Relat Res*. 2023;25(2): 370-380. doi:10.1111/cid.13184